Hypoglycemia leads to age-related loss of vision

Y. Umino*, D. Everhart*, E. Solessio*, K. Cusato*†, J. C. Pan*, T. H. Nguyen*, E. T. Brown*, R. Hafler*, B. A. Frio*, B. E. Knox*, G. A. Engbretson*†, M. Haeri*, L. Cui‡, A. S. Glenn‡, M. J. Charron‡, and R. B. Barlow*§

*Center for Vision Research, Department of Ophthalmology, State University of New York Upstate Medical University, Syracuse, NY 13210; ‡Department of Biochemistry, Albert Einstein College of Medicine, Bronx, NY 10461; and †Department of Biomedical and Chemical Engineering, Syracuse University, Syracuse, NY 13244

Edited by John E. Dowling, Harvard University, Cambridge, MA, and approved November 1, 2006 (received for review May 31, 2006)

The retina is among the most metabolically active tissues in the body, requiring a constant supply of blood glucose to sustain function. We assessed the impact of low blood glucose on the vision of C57BL/6J mice rendered hypoglycemic by a null mutation of the glucagon receptor gene, *Gcgr*. Metabolic stress from moderate hypoglycemia led to late-onset loss of retinal function in Gcgr$^{-/-}$ mice, loss of visual acuity, and eventual death of retinal cells. Retinal function measured by the electroretinogram b-wave threshold declined >100-fold from age 9 to 13 months, whereas decreases in photoreceptor function measured by the ERG a-wave were delayed by 3 months. At 10 months of age Gcgr$^{-/-}$ mice began to lose visual acuity and exhibit changes in retinal anatomy, including an increase in cell death that was initially more pronounced in the inner retina. Decreases in retinal function and visual acuity correlated directly with the degree of hypoglycemia. This work demonstrates a metabolic-stress-induced loss of vision in mammals, which has not been described previously. Linkage between low blood glucose and loss of vision in mice may highlight the importance for glycemic control in diabetics and retinal diseases related to metabolic stress as macular degeneration.

C57BL/6J mice | cell death | glucagon receptor gene | retinal function | visual acuity

Changes in metabolism can affect vision. Lowering blood glucose (BG) can decrease human visual sensitivity (1–3) as does reducing the partial pressure of inhaled oxygen (4). Natural nighttime decreases in glucose availability (5, 6) parallel a decline in visual sensitivity that can be restored by glucose ingestion (7). In the cat, acute decreases in glucose supply can transiently reduce retinal sensitivity (8) and exacerbate the effects of hypoxia on the retina (9). The effects of metabolite supply on vision are not surprising in view of the high energy consumption by the retina (10, 11). Although the retina's high metabolic activity has been known for >40 years (12), the consequences of an inadequate supply of metabolites are not completely understood.

We report here that a chronic decrease in BG in mice decreases retinal function, leading to a loss of vision and eventual degeneration of the retina. We observed decreases in both electroretinogram (ERG) a- and b-waves, as well as a loss in visual acuity. Retinal cell death, assayed by TUNEL, was increased in Gcgr$^{-/-}$ mice, and decreases in cell number were detected. These data indicate that a chronic decrease in BG leads to loss of vision and cell death in mice and highlight the possibility that the human retina may likewise be susceptible to hypoglycemia.

Results

Glucagon Receptor and Changes in BG. Hypoglycemia was induced in C57BL/6J mice by a null mutation of the glucagon receptor gene, *Gcgr* (13). Among its actions, the glucagon receptor under control of glucagon regulates gluconeogenesis to increase BG levels. Liver and kidney abundantly express *Gcgr*, and PCR analysis reveals trace levels of receptor mRNA in the retina of wild-type (WT) mice (14), a result we confirm (data not shown). Adult Gcgr$^{-/-}$ mice exhibited a BG range of 50–115 mg/dl (see *Methods*) with a mean ± SD of 78.4 ± 16.9 mg/dl (11–13 months of age, $n = 14$). In several tests reported here we divided the mice into moderately (<95 mg/dl; average = 70.6 ± 12.2; $n = 9$) and mildly (>95 mg/dl; 91.0 ± 16.2; $n = 5$) hypoglycemic groups. Age-matched WT and littermate Gcgr$^{+/-}$ mice had average BG of 126.9 ± 21.5 mg/dl ($n = 11$) and 129.1 ± 22.4 mg/dl ($n = 9$), respectively. We analyzed vision of these three genotypes as a function of age.

Table 1. Summary of ERG parameters from Gcgr$^{-/-}$ mice

Age, months	a-wave			b-wave		
	Log I_t	Log I_0	V_{max}, μV	log I_t	log I_0	V_{max}, μV
≤8	−0.9	0.1 ± 0.1	230 ± 10	−3.8	−2.4 ± 0.1	470 ± 20
9	−0.9	−0.2 ± 0.1	160 ± 10	−3.3	−2.1 ± 0.1	420 ± 20
10	−1.0	−0.2 ± 0.2	160 ± 20	−2.9	−2.0 ± 0.1	310 ± 10
11	−0.7	NT	NT	−2.9	−2.3 ± 0.3	200 ± 20
12	−0.4	−0.2 ± 0.1	90 ± 10	−2.2	−1.7 ± 0.3	180 ± 30
13	−0.4	−0.3 ± 0.6	80 ± 60	−1.8	−2.1 ± 0.4	100 ± 30

Data are mean ± SEM; $n = 4$–12; V_{max}, maximum amplitude; NT, not tested.

Losses in Retinal Function. The earliest detectable change in vision of hypoglycemic Gcgr$^{-/-}$ mice is a loss of retinal function. We assessed their retinal function by recording the ERG (Fig. 1*A*). The corneal negative a-wave of the ERG yields information about phototransduction processes and precedes the corneal positive b-wave that reflects postphototransduction responses. The a- and b-waves recorded from 8-month-old Gcgr$^{-/-}$ mice (Fig. 1*A*, red trace) have the same amplitudes and kinetics as those recorded from same-age euglycemic Gcgr$^{+/-}$ mice (Fig. 1*A*, black trace), indicating equal retinal sensitivities. However, both a- and b-waves were substantially smaller at 13 months of age, indicating large losses in retinal function of older hypoglycemic mice. The systematic age-related changes in the ERG components are evident in the intensity-response functions plotted in Fig. 1 *B* and *C* and Table 1. Note that the threshold intensities for evoking b-waves progressively increased for Gcgr$^{-/-}$ mice 9 months of age and older, whereas those for a-waves increased only in 12- to 13-month-old mice.

We tracked the age-related changes in retinal function by

Author contributions: Y.U., D.E., E.S., B.E.K., and R.B.B. designed research; Y.U., D.E., E.S., K.C., J.C.P., T.H.N., E.T.B., R.H., B.A.F., G.A.E., and M.H. performed research; L.C., A.S.G., and M.J.C. contributed new reagents/analytic tools; Y.U., D.E., E.S., J.C.P., T.H.N., and R.B.B. analyzed data; and Y.U., D.E., K.C., and R.B.B. wrote the paper.

The authors declare no conflict of interest.

This article is a PNAS direct submission.

Freely available online through the PNAS open access option.

Abbreviations: BG, blood glucose; ERG, electroretinogram; INL, inner nuclear layer; ONL, outer nuclear layer; IPL, inner plexiform layer; OPL, outer plexiform layer.

§To whom correspondence should be addressed at: Center for Vision Research, Department of Ophthalmology, 3258 Weiskotten Hall, 750 East Adams Street, SUNY Upstate Medical University, Syracuse, NY 13210. E-mail: barlowr@upstate.edu.

This article contains supporting information (SI) online at www.pnas.org/cgi/content/full/0604478104/DC1.

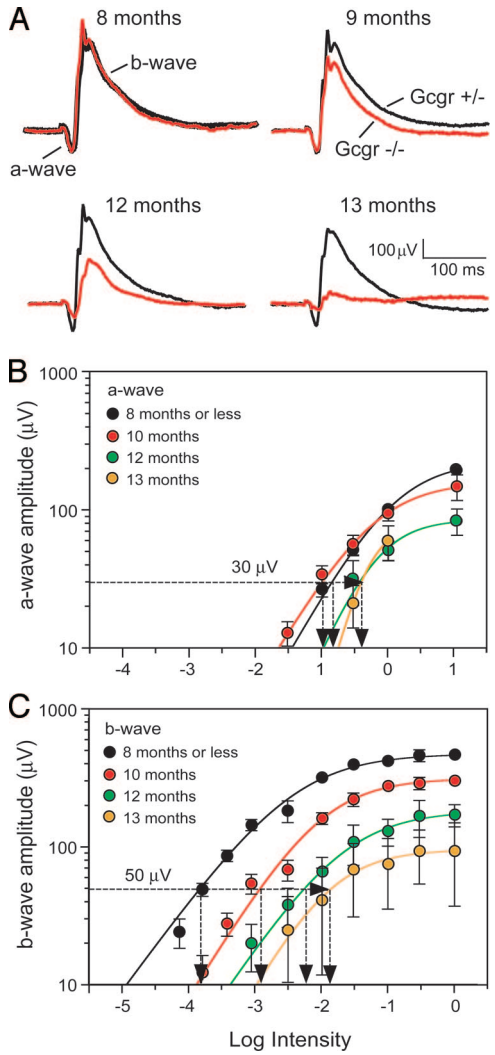

Fig. 1. Age-related changes in the ERG. (*A*) Average ERGs recorded from a group of moderately hypoglycemic Gcgr$^{-/-}$ mice (red traces; $n = 3$) and euglycemic Gcgr$^{+/-}$ mice (black traces; $n = 4$) in response to 10-ms flashes. (*B*) Intensity-response functions of a-waves recorded from moderately hypoglycemic Gcgr$^{-/-}$ mice ages ≤8 to 13 months. (*C*) Intensity-response functions of b-waves from the same ERGs that yielded the a-waves in *B*. Dashed horizontal lines and vertical intercepts on the abscissa show the method for determining threshold light intensities (I_t). Responses in *B* and *C* were recorded at ≤8, 10, 12, and 13 months from 12, 17, 7, and 4 Gcgr$^{-/-}$ mice, respectively.

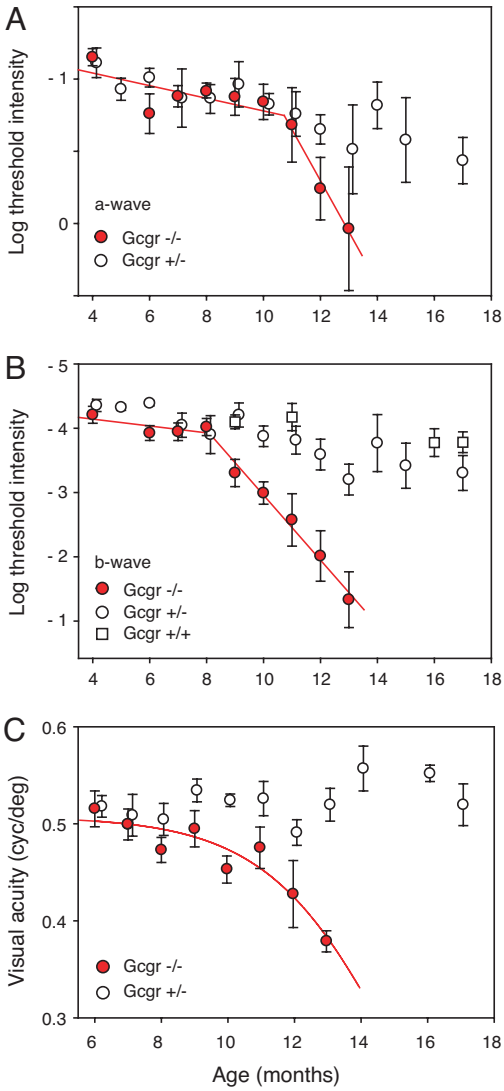

Fig. 2. Tracking changes in retinal function and visual acuity. (*A*) Phototransduction (a-wave) activity of moderately hypoglycemic Gcgr$^{-/-}$ mice (red symbols) and euglycemic Gcgr$^{+/-}$ mice (open circles; $n = 6–8$) as a function of age. Euthanization of older Gcgr$^{-/-}$ mice for retinal histology limited sample size at 9, 10, 11, 12, and 13 months to 13, 12, 10, 7, and 4 mice, respectively. The large spread of data at 13 months results from small sample size ($n = 4$) and lack of ERG from one mouse. (*B*) Age-related changes in postphototransduction (b-wave) response (see *Methods*) of the same group of Gcgr$^{-/-}$ and Gcgr$^{+/-}$ mice plus Gcgr$^{+/+}$ mice (open squares; $n = 4–6$). Red line segments are least-squares fits. (*C*) Visual acuity of moderately hypoglycemic Gcgr$^{-/-}$ mice (red symbols) and euglycemic littermate Gcgr$^{+/-}$ mice (open circles; $n = 3–8$). Euthanization for histology limited the data at 11, 12, and 13 months to 9, 7, and 5 mice, respectively. Red curve is a polynominal fit. Median illumination at the surface of the cornea was 70 cdm^{-2}. Bars are SEM.

periodically measuring the threshold light intensities (I_t) required to evoke small-amplitude a- and b-waves, 30 and 50 μV, respectively. Plotting retinal I_t as a function of age shows that a-wave threshold intensity begins to increase at ≈12 months of age (Fig. 2*A*, red symbols). The b-wave threshold of the same mice begins to change earlier at 9 months of age, increasing >100-fold over the next 4 months (Fig. 2*B*). That of euglycemic Gcgr$^{+/+}$ and Gcgr$^{+/-}$ mice remained relatively stable, increasing only ≈3-fold from 4 to 17 months of age.

Loss of retinal function in hypoglycemic Gcgr$^{-/-}$ mice is not associated with significant changes in the kinetic properties of the ERG. The latency of the b-wave response is approximately the same for both genotypes, suggesting that initial losses result from local rather than global changes in retinal function [see supporting information (SI) Fig. 5]. Minimal age-related changes in the intensity for half-maximal b-wave response (I_o) also suggest local changes in retinal function. Table 1 summarizes ERG parameters recorded from Gcgr$^{-/-}$ mice. Experiments in Figs. 1 and 2 were carried out under dark-adapted conditions that favor rod-mediated responses. To assess cone-mediated responses, we recorded ERGs by using a paired-flash paradigm and found that cone responses of Gcgr$^{-/-}$ mice declined at the same rate as rod responses (see SI Fig. 6). The progressive age-related losses in the ERG suggest that hypoglycemia equally affects both rod- and cone-mediated responses and acts earlier on cellular mechanisms downstream from phototransduction (b-wave) than on phototransduction processes themselves (a-wave). The initial site(s) of action could be the photoreceptor synapse or retinal cells postsynaptic to the photoreceptors.

Losses in Visual Acuity. Age-related losses in visual acuity of hypoglycemic mice lag behind those in retinal function (Fig. 2*C*). Visual acuity of moderately hypoglycemic Gcgr$^{-/-}$ mice (red symbols) began to decline at 10 months of age and continued until age 13 months, when the mice were killed for retinal histology. Euglycemic littermate Gcgr$^{+/-}$ mice maintained high visual acuities past 16 months of age. We measured visual acuities of mice by observing their optomotor behavior in response to rotating sinusoidal patterns using a double-blind procedure (see *Methods*).

Blood Glucose. We investigated whether BG level is the independent variable mediating vision loss. Not all Gcgr$^{-/-}$ mice are equally hypoglycemic, and not all Gcgr$^{+/+}$ and Gcgr$^{+/-}$ mice are equally euglycemic. To test the role of glucose, we grouped all adult mice (10–13 months old) according to their BG phenotype and plotted their retinal thresholds and visual acuity as functions of BG level (Fig. 3 *A* and *B*). The near-linear relationships between BG and these measures of vision indicate that BG is a strong predictor of losses in vision.

To further test the role of BG, we placed Gcgr$^{-/-}$ mice on a high-carbohydrate diet that elevated BG to euglycemic levels (129.2 ± 9.0 mg/dl, $n = 5$). We selected 6- to 7-month-old mice that had not yet experienced a loss of vision. Fig. 3*C* shows that maintaining these mice at euglycemic levels retained near normal retinal response past the age of 12 months when they would normally have had a substantial loss of vision. Not only is BG a predictor of vision loss, but restoration of euglycemic BG delays loss of vision.

We investigated whether the loss of vision is simply a function of decreased availability of glucose. Acute hyperglycemia (206 ± 40 mg/dl) caused by dextrose ingestion in 13-month-old Gcgr$^{-/-}$ mice (see *Methods*) produced no concomitant increase in retinal response as measured by the ERG b-wave amplitude and threshold intensity ($n = 3$; data not shown). Neither ERG measure was affected by transient increases in BG. We conclude that acute increases in glucose availability are not enough to rescue retinal responses and suggest that the loss of retinal function in Gcgr$^{-/-}$ mice is not reversible.

Changes in Retinal Anatomy. Histological analysis showed that age-related changes in retinal anatomy of hypoglycemic mice occur later than those in visual acuity and retinal function (Fig. 4). The changes are generally small and are first detectable in mice at ≈10–11 months of age. Comparing axial sections of retinas from all three genotypes reveals a slight thinning of the major retinal layers of the retina of a 13-month-old Gcgr$^{-/-}$ mouse. The analyses in Fig. 4 *B–D* of the outer nuclear layers (ONLs) and inner nuclear layers (INLs) show that Gcgr$^{-/-}$ mice lost 8% of ONL cells relative to WT and 6.4% of ONL cells relative to Gcgr$^{+/-}$ mice. The ONL contains cell bodies of rod and cone photoreceptors. Although the ONL in Gcgr$^{-/-}$ mice contains fewer cell bodies, the remaining photoreceptors appear to have normal structures from the tip of the outer segment of photoreceptor (OS) to the outer plexiform layer (OPL). Also, adult Gcgr$^{-/-}$ mice have ≈12% fewer INL cells than Gcgr$^{+/+}$ and Gcgr$^{+/-}$ mice. With respect to the synaptic layers [inner plexiform layer (IPL) and OPL], note that the OPL of the Gcgr$^{-/-}$ mouse in Fig. 4*A* appears thinner than that of Gcgr$^{+/+}$ and Gcgr$^{+/-}$ mice, but the change may not be significant.

The small changes in retinal anatomy of hypoglycemic relative to euglycemic mice are remarkable in light of the accompanying changes in retinal function. For example, the 13-month-old Gcgr$^{-/-}$ mice had a 100-fold loss in retinal response (b-wave threshold; Fig. 2*B*) with only modest losses of cells in the ONL and INL (Fig. 4 *B* and *C*). Several of the Gcgr$^{-/-}$ mice we examined exhibited extensive degeneration with few cells remaining in both the ONL and INL or had patches of retina missing completely with some adhering to the posterior surface of the lens. Such mice were functionally blind with no recordable ERGs. Their data are not included in the analyses in Fig. 4.

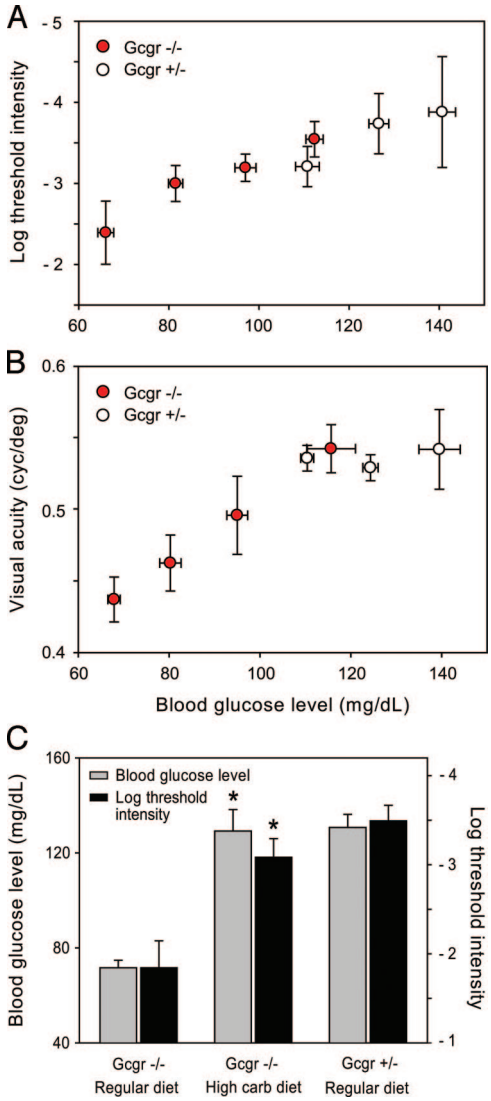

Fig. 3. BG independently modulates retinal and visual function. (*A* and *B*) Retinal response threshold (*A*) and visual acuity (*B*) plotted as functions of BG of Gcgr$^{-/-}$ and Gcgr$^{+/-}$ mice. Results were averaged according to BG levels by clustering BG levels into six bins (15 mg/dl wide) from 60 to 150 mg/dl. Data were acquired from 17 Gcgr$^{+/-}$ and 14 Gcgr$^{-/-}$ mice (*A*) and from 11 Gcgr$^{+/-}$ and 10 Gcgr$^{-/-}$ mice (*B*) with up to four trials per mouse. (*C*) Comparison of retinal response thresholds of Gcgr$^{-/-}$ and Gcgr$^{+/-}$ mice maintained on a regular diet with Gcgr$^{-/-}$ mice placed on a high-carbohydrate diet beginning at 6–7 months of age ($n = 5$–7). Gcgr$^{-/-}$ mice on a high-carbohydrate diet were significantly different from Gcgr$^{-/-}$ mice on regular diet (*, $P < 0.05$, one-way ANOVA; Holm–Sidak test). Bars are SEM.

Cell Death. Retinal cell death is elevated in older hypoglycemic mice. TUNEL-positive cells were detected in the Gcgr$^{-/-}$ mouse retina. The section in Fig. 4*A* contains an exceptional number of positive cells and emphasizes our general finding of cell death being initially more pronounced in the proximal INL portion of the retina before occurring in the outer retina. The summary of TUNEL across all three genotypes (Fig. 4*D*) reveals more dying cells in the retinas of Gcgr$^{-/-}$ mice. Only 6.4% of TUNEL-positive cells colabeled with cleaved caspase-3 (data not shown). These results suggest a caspase-3-independent pathway to cell death (15).

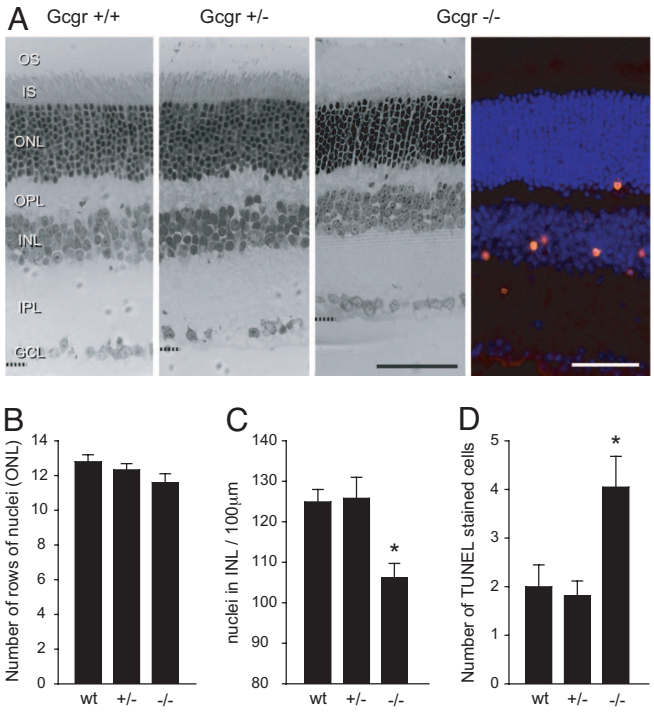

Fig. 4. Progressive changes in retinal anatomy. (*A*) Light micrographs of axial plastic-embedded sections of retinas from age-matched adult $Gcgr^{+/+}$, $Gcgr^{+/-}$, and moderately hypoglycemic $Gcgr^{-/-}$ mice (leftmost three sections; 1-μm thick). Shown are photoreceptors (outer segments, OS; inner segments, IS) at the top and the ganglion cell layer (GCL) at the bottom. Visible in between are the OPL and IPL and the densely stained cell bodies in the ONL and INL. The oblique cryosection on the right from a $Gcgr^{-/-}$ mouse shows TUNEL staining primarily in the INL. The different fixation methods caused differential tissue shrinkage. (Scale bars: 50 μm.) (*B*) Numbers of rows of cell nuclei counted in ONL of $Gcgr^{+/+}$ ($n = 5$), $Gcgr^{+/-}$ ($n = 6$), and $Gcgr^{-/-}$ ($n = 7$) mice are not significantly different. (*C*) Numbers of INL cells counted within 100-μm horizontal sectors are significantly fewer for $Gcgr^{-/-}$ mice than for $Gcgr^{+/+}$ and $Gcgr^{+/-}$ mice. (*D*) Average number of TUNEL-positive cells is significantly greater (*, $P < 0.05$) for $Gcgr^{-/-}$ mice ($n = 12$) than for $Gcgr^{+/+}$ ($n = 8$) and $Gcgr^{+/-}$ ($n = 11$) mice.

Discussion

To summarize, hypoglycemic $Gcgr^{-/-}$ mice exhibit age-related losses in retinal function followed by losses in visual acuity and cell death in the inner retina (INL). Euglycemic $Gcgr^{+/+}$ and $Gcgr^{+/-}$ mice maintain high acuity with small decreases in retinal responses over the 17-month testing period. Others had noted age-related losses in retinal responses of WT C57BL/6J mice. Gresh *et al.* (16) reported decreases in the ERG b-wave amplitude accompanied by cell loss in the outer retina (ONL) as mice aged from 4 to 17 months. Li *et al.* (17) also found decreases in ERG amplitude as WT pigmented mice aged from 2 to 12 months, but they did not report a corresponding change in retinal anatomy.

Vision losses in hypoglycemic mice are distinguished by their late onset (>8 months) and slow rate (>5 months). Typically, retinal degeneration in transgenic mice begins at or shortly after birth and is complete in a matter of weeks (18). However, there are exceptions such as $Rds^{-/-}$ mice in which retinal degeneration begins early in life but continues slowly for months (19). Also, mice deficient in either the monocyte chemoattractant protein ($Ccl2^{-/-}$) or the chemokine receptor-2 ($Ccr2^{-/-}$) exhibit late-onset degeneration, beginning at ≈9 months of age and progressing over the next 3–4 months (20). Interestingly, these temporal properties approximate those that we report here for $Gcgr^{-/-}$ mice.

Cell death occurring initially in the INL of the retina of $Gcgr^{-/-}$ mice differs from the common observation of degeneration beginning in the outer layers, specifically the photoreceptor layer, as a result of null mutations of genes involved primarily in photoreceptor function (21). An exception is the harlequin mutant mouse (*Hq*) in which retinal cell death initially occurs in the inner layers with eventual involvement of all retinal layers (22). Although degeneration is associated with a proviral insertion mutation in a gene encoding Apoptosis Inducing Factor, the precise molecular mechanism(s) are not known. The mechanisms underlying cell death in $Gcgr^{-/-}$ retinas are also not known, but our results point to caspase-3-independent mechanisms.

Extent of cell death (Fig. 4) is modest in comparison with the substantial losses in retinal function. A possible explanation is that initially metabolically stressed cells lose function irreversibly without undergoing apoptosis. Such nonfunctioning cells may persist with near normal anatomy despite their inability to signal changes in the visual field. Alternatively, such nonfunctioning cells may exist in a dormant state that can be rescued with prolonged exposure to euglycemic conditions. Either way, the point at which cell function is lost may be well upstream of apoptosis.

Dependence of vision loss on BG level (Fig. 3) suggests that it is not a direct result of the null mutation of *Gcgr* but rather a consequence of the metabolic stress from hypoglycemia caused by the mutation. Because glucose is essential for retinal function, an inadequate supply may lead to a subnormal production of ATP and eventual cell death. Glucose metabolism dysfunction has been linked to impaired vision and loss of retinal function in zebrafish (23). Links between glucose metabolism and cell death are beginning to be worked out in other tissues (24). In $Gcgr^{-/-}$ mice the events triggered by systemic hypoglycemia are not known. They may act alone or in concert with other processes such as oxidative stress that is known to be associated with retinal cell death (25) and may impair vision by altering brain as well as retinal function.

Recurrent hypoglycemia is the most feared complication of intensive insulin treatment of type 1 diabetes (26). It causes disabling episodes and recurrent morbidity in most type 1 diabetics as well as many type 2 diabetics and can be fatal. Chronic hypoglycemia, as we report here, causes loss of vision and eventual retinal degeneration in mice. These actions of recurrent and chronic hypoglycemia may further underscore the importance of glycemic control by diabetics.

Materials and Methods

Animals. Mice possessing a null mutation of the glucagon receptor ($Gcgr^{-/-}$) were generated as described (13). We studied mice that were backcrossed onto the C57BL/6J background, as well as littermate controls and age-matched WT mice. Mutant alleles were confirmed by PCR analysis. Mice on regular diet were fed Formulab Diet (catalog no. 5008; Purina, St. Louis, MO) ad libitum and maintained on a 14-h/10-h light/dark cycle. Mice on the high-carbohydrate diet were fed Purina High Carbohydrate Purified Diet (catalog no. 46249) ad libitum with the same light/dark cycle. We tested both male and female mice. BG levels were measured from the tail vein with a OneTouch Ultra glucose meter (LifeScan, Milpitas, CA). Protocols were approved by the Institutional Animal Care and Use Committee at SUNY Upstate Medical University.

Retinal Function. We assessed retinal function by recording the ERG (27). Dark-adapted mice were placed in a light-proof cage before light onset (0800 h) and anesthetized with Nembutal (5 mg/ml: 60 mg/kg; ref. 28); their pupils were dilated with Tropicamide, their corneas were kept moist with 0.3% glycerin/1.0% propylene glycol, and their body temperature was maintained at

37°C with a heating pad. ERGs were recorded on a Burian Allen electrode (Hansen Ophthalmic Development Lab, Coralville, IA; 0.3–1,000 Hz) in response to 10-ms LED flashes (520 nm) that delivered 55 cdsm^{-2} (0.9×10^5 photons μm^{-2}) at the surface of the cornea at log $I = 0$. The a-wave amplitude was measured from baseline to the trough of the initial corneal negative wave; b-wave was measured from the a-wave trough to the peak of the corneal positive wave. Plotted as a function of light intensity on log-log coordinates in Fig. 1, the amplitudes of the a- and b-waves were fitted with Hill function, and threshold intensities, indicated by I_t, required to evoke 30-μV a-waves and 50-μV ERG b-waves were determined. Retinal function was also measured by determining the light intensity necessary to evoke a half-maximal b-wave, I_o. Temporal properties of the ERG were measured by the latency from light flash to the peak of the b-wave, the so-called implicit time. Cone contributions to the ERG were determined by using a paired-flash paradigm (see SI Fig. 6). Conditions of acute hyperglycemia were induced by delivering 150–200 μl of 50% dextrose solution via a polyethylene tube (o.d. = 750 μm) to the stomach while the mouse was under anesthesia. ERGs were recorded after BG changes plateaued (≈30 min).

Visual Acuity. We measured visual acuity of mice by observing their optomotor behavior using two-alternative forced-choice in combination with a computer-controlled display (OptoMotry; refs. 29 and 30). The optomotor stimulus was a vertically oriented sinusoidal pattern (100% contrast) rotated for 5-s periods at a speed of 12^0/sec under photopic luminance levels (peak-to-peak luminance: 0.36–154.5 cd m^{-2}). Our double-blind protocol ensured that the experimenter was unaware of the age, sex, and genotype of the tested animal and the direction of rotation of the sinusoidal pattern presented to the animal. The two-alternative forced-choice method required the observer to choose the direction of pattern rotation based only on the animal's behavior. Auditory feedback indicates correct/incorrect observer responses with threshold set equal to 70% correct. Each measure of visual acuity is the mean of four trials. Mice were tested under photopic conditions during the first 4 h of their daytime light cycle.

Histology. Anesthetized mice were perfused by intracardiac injection with PBS (pH 7.4) and then 4% paraformaldehyde in 0.1 M phosphate buffer (PB). The eyes were enucleated and post-fixed in 1% OsO_4/2% paraformaldehyde/1.25% glutaraldehyde in PBS (1 h) and then embedded in epoxy medium. Vertical sections (1-μm thick) were cut through the center of the eye and stained with toluidine blue for light microscopy.

TUNEL and Immunohistochemistry. Animals were anesthetized, and their eyes were enucleated and fixed in 4% paraformaldehyde (4 h). Tissue was then cryoprotected in 30% sucrose overnight, embedded in OCT compound, and sectioned with a cryostat at 16 μm. Sequential vertical sections cut through the center of the eye were labeled by TUNEL (Promega, Madison, WI) following the manufacturer's instructions. Tyramide-Cy3 (PerkinElmer, Wellesley, MA) was used instead of the colorimetric substrate for detection. After TUNEL, slides were immunolabeled with rabbit polyclonal antibodies to the cleaved subunit of caspase-3 (Cell Signaling Technology, Beverly, MA; 1:50) by using Cy2-conjugated goat anti-rabbit (Jackson ImmunoResearch, West Grove, PA) as a secondary and counterstained with DAPI (Molecular Probes, Eugene, OR). Using fluorescence microscopy, we examined the retinas of all three genotypes and scored individual TUNEL-positive and cleaved caspase-3 immunopositive cells. Averages were computed for Gcgr$^{+/+}$ ($n = 8$), Gcgr$^{+/-}$ ($n = 11$), and Gcgr$^{-/-}$ ($n = 12$) mice by summing the positive-stained cells in the five sequential sections cut vertically through the center of the eye and dividing the sum by five. Adjacent sections were stained with toluidine blue for light microscopy.

We thank Thomas Loi, Nyla Abassi, and Payam Amini for technical assistance, Robert Sherwin for helpful suggestions, and Robert Quinn and the staff at SUNY Health Center Animal Resources for animal husbandry. This work was supported by the Nationals Institutes of Health (R.B.B., M.J.C., and B.E.K.), the American Diabetes Association, AECOM Comprehensive Cancer Center (M.J.C.), the National Aeronautics and Space Administration (R.B.B.), Fight for Sight (D.E.), Research to Prevent Blindness, and the Lions of Central NY.

1. McFarland RA, Halperin MH, Niven JI (1945) *Am J Physiol* 144:378–388.
2. Tabandeh H, Ranganath L, Marks V (1996) *Eur J Ophthalmol* 6:81–86.
3. McGrimmon RJ, Deary IJ, Huntly BJP, MacLeod KJ, Frier BM (1996) *Brain* 119:1277–1287.
4. McFarland RA, Forbes WH (1940) *J Gen Physiol* 24:69–98.
5. Clore J, Nestler J, Blackard W (1989) *Diabetes* 38:285–290.
6. Van Cauter E, Blackman JD, Roland D, Spire JP, Refetoff S, Polonsky KS (1991) *J Clin Invest* 88:934–942.
7. Barlow RB, Khan M, Farell B (2003) *Adv Exp Med Biol* 533:259–267.
8. Macaluso C, Onoe S, Niemeyer G (1992) *Invest Opthalmol Visual Sci* 33:2798–2807.
9. Kang Derwent JJ, Linsenmeier RA (2001) *Visual Neurosci* 18:983–993.
10. Ames A III, Li YY, Heher EC, Kimble CR (1992) *J Neurosci* 12:840–853.
11. Winkler BS (1981) *J Gen Physiol* 77:667–692.
12. Ames A III, Gurian BS (1963) *J Neurophysiol* 26:617–634.
13. Gelling RW, Du XQ, Dichmann DS, Romer J, Huang H, Cui L, Obici S, Tang B, Holst JJ, Fledelius C, *et al.* (2003) *Proc Natl Acad Sci USA* 100:1438–1443.
14. Feldkaemper MP, Burkhardt E, Schaeffel F (2004) *Exp Eye Res* 79:321–329.
15. Doonan F, Donovan M, Cotter TG (2003) *J Neurosci* 23:5723–5731.
16. Gresh J, Goletz PW, Crouch RK, Rohrer B (2003) *Visual Neurosci* 20:211–220.
17. Li C, Cheng M, Yang H, Peachey NS, Naash MI (2001) *Optometry Vision Sci* 78:425–430.
18. Pacione LJ, Szego MJ, Ikeda S, Nishina PM, McInnes RR (2003) *Annu Rev Neurosci* 26:657–700.
19. Sanyal S, De Ruiter A, Hawkins RK (1980) *J Comp Neurol* 194:193–207.
20. Ambati J, Anand A, Fernandez S, Sakurai E, Lynn BC, Kuziel WA, Rollins BJ, Ambati BK (2003) *Nat Med* 9:1390–1397.
21. Dryja TP, McGee TL, Reichel E, Hahn LB, Cowley GS, Yandell DW, Sandberg MA, Berson EL (1990) *Nature* 343:364–366.
22. Klein JA, Longo-Guess CM, Rossmann MP, Seburn KL, Hurd RE, Frankel WN, Bronson RT, Ackerman SL (2002) *Nature* 419:367–374.
23. Brockerhoff SE, Hurley JB, Janssen-Bienhold U, Neuhauss SC, Driever W, Dowling JE (1995) *Proc Natl Acad Sci USA* 92:10545–10549.
24. Danial NN, Gramm CF, Scorrano L, Zhang CY, Krauss S, Ranger AM, Datta SR, Greenberg ME, Licklider LJ, Lowell BB, *et al.* (2003) *Nature* 424:952–956.
25. Age-Related Eye Disease Study Research Group (2001) *Arch Ophthalmol* 119:1417–1436.
26. Cryer PE (2004) *N Engl J Med* 350:2272–2279.
27. Dowling JE (1960) *Am J Ophthalmol* 50:875–889.
28. Brown ET, Umino Y, Loi T, Solessio E, Barlow R (2005) *Visual Neurosci* 22:615–618.
29. Prusky GT, Alam NM, Beekman S, Douglas RM (2004) *Invest Ophthalmol Visual Sci* 45:4611–4616.
30. Umino Y, Frio B, Abbasi M, Barlow R (2006) *Adv Exp Med Biol* 572:169–172.